Contents lists available at ScienceDirect

Chemical Engineering Research and Design

journal homepage: www.elsevier.com/locate/cherd

Multi-scale modeling of granulation processes: Bi-directional coupling of PBM with DEM via collision frequencies

*Dana Barrasso, Rohit Ramachandran**

Department of Chemical and Biochemical Engineering, Rutgers, The State University of New Jersey, Piscataway, NJ 08854, USA

ABSTRACT

Wet granulation is a complex particle design process often operated inefficiently in industrial applications. Enhanced process understanding is required to facilitate design, control, and optimization. In this study, a hybrid multi-scale model is presented using a bi-directional coupling approach between DEM and PBM. The hybrid model takes into account particle collision frequencies and liquid distribution, providing a framework suitable for the complex sub-processes in wet granulation. The effect of particle size distribution on the collision frequency function was demonstrated, indicating the need for a multi-scale model. Results of the hybrid model show an increase in particle size over time from an average diameter of 0.98 mm to 2.5 mm, which qualitatively agrees with experimental trends observed during the liquid addition and wet massing stages. Two-dimensional distributions in particle size and liquid fraction are also presented incorporating the key effect of liquid distribution on the evolution of granule PSD.

Keywords: Granulation; Population balance modeling; Discrete element modeling; Multi-scale model; Aggregation; Collision rate

1. Introduction

Granulation is a particle design process used to create larger granules from fine powder, improving flowability, compactibility, and homogeneity while reducing dust formation. Although it is widely used in the food, pharmaceutical, detergent, and fertilizer industries, it is often operated inefficiently, with high recycle ratios in continuous processes and high rejection rates in batch processes (Wang and Cameron, 2002). The design and control of granulation processes is primarily performed via heuristic experimentation, and a more mechanistic approach is required to improve operational efficiency (Cameron et al., 2005).

The wet granulation process is highly complex, governed by the rate processes of wetting and nucleation, aggregation and consolidation, and breakage and attrition (Iveson et al., 2001). In wetting and nucleation, the fine powder comes into contact with the liquid binder and forms granule nuclei. When wet particles collide, they can form liquid bridges, resulting in aggregation. Collisions with vessel walls and/or impellers also result in consolidation, leading to a reduction in the porosity of a granule. Breakage and attrition occur when large particles are subjected to shear, compressive, and tensile forces and break to form fragments.

Based on these sub-processes, a single granule can be described by three internal properties. The size, related to the solid volume, is a critical product attribute. The liquid content, related to the amount of liquid within and on the surface of a particle, affects the aggregation rate. The porosity, related to the air volume, affects the surface liquid and as it decreases, liquid is forced out of the pores and onto the particles, further affecting aggregation rates (Cameron et al., 2005). The product porosity also affects the compactibility of the granules, which is critical to tablet manufacturing (Vervaet and

* *Corresponding author*. Tel.: +1 848 445 6278; fax: +1 732 445 2581.
E-mail address: rohit.r@rutgers.edu (R. Ramachandran).

Available online 28 April 2014
http://dx.doi.org/10.1016/j.cherd.2014.04.016

Remon, 2005). In multi-component granulation processes, the composition of each granule is also important, and segregation can occur, affecting the final product (Vervaet and Remon, 2005).

In the pharmaceutical industry, recent efforts focus on implementing Quality by Design (QbD). QbD involves developing a strong process understanding and defining a design space, a set of operating parameters that will result in a quality product Yu (2008). In contrast, a Quality by Testing (QbT) approach involves sampling the products of empirically designed processes and rejecting batches that do not meet specifications, often wasting expensive active ingredients. Current research and development efforts aim to shift from batch to continuous processing in tablet manufacturing in order to improve controllability, scalability, and profitability. In order to successfully transition to continuous processing, a QbD approach is desired, and a more mechanistic understanding of powder processes is needed.

To meet these challenges, a model-based approach has been proposed, where empirical and mechanistic models are developed and validated using experimental data (Glaser et al., 2009; Ramachandran and Chaudhury, 2012). Validated models can then be used as predictive tools to aid in design, model-based control, and optimization. Various modeling approaches have been employed for granulation. Data-driven models include response surface methodology (RSM) and artificial neural networks (ANN) (Ranjbarian and Farhadi, 2013; Behzadi et al., 2005). These models use data from existing or experimental processes, and have limited ability to predicting process behavior beyond the experimental space. Population balance models (PBMs) provide a more fundamental framework for tracking changes in particle properties over time, though they require rate expressions and empirical parameters that cannot easily be measured. Discrete element modeling (DEM) is more mechanistic, tracking particles as they move through space and collide. However, DEM by itself does not account for aggregation or other rate processes involved in wet granulation. Further, computational fluid dynamics (CFD) can also be used to determine drag forces resulting from fluid flow, which are significant in fluid bed granulation processes. Along with DEM, these forces can be used to determine particle fluxes.

In this study, a multi-scale model is presented, solving a two-dimensional PBM within a DEM simulation, focusing on systems such as high-shear, twin-screw, and drum granulation, which do not incorporate an air flow stream (such as in fluid bed granulation). As a result, CFD aspects can be neglected.

1.1. Objectives

The purpose of this study is to develop a coupled PBM–DEM model for wet granulation processes, with the following objectives:

- Demonstrate the limitations of PBM and DEM when used independently to model granulation processes.
- Present a hybrid PBM–DEM model using two-way coupling to transfer data related to collision frequencies and size and liquid distribution.
- Propose a framework for future work to incorporate additional sub-processes and complexities within the hybrid model.

2. Background

The PBM groups particles into classes based on properties such as size and wetness and tracks the change in the number of particles in each class over time. In contrast, DEM tracks each individual particle as it moves through space and collides with other objects. Both modeling techniques have been applied extensively to granulation processes.

2.1. Population balance modeling

The PBM is a class of integro-differential equations that describe the change in the number of particles within each class over time as the particles are subjected to rate processes, such as liquid addition, consolidation, aggregation, and breakage. A general form of the population balance equation is given in Eq. (1) (Ramkrishna, 2000).

$$\frac{dF(\mathbf{x},t)}{dt} + \frac{\partial}{\partial \mathbf{x}}\left[F(\mathbf{x},t)\frac{d\mathbf{x}}{dt}(\mathbf{x},t)\right] = \Re_{formation}(\mathbf{x},t) - \Re_{depletion}(\mathbf{x},t) \quad (1)$$

Here, F represents the number of particles or particle density as a function of particle class and time. The set of particle properties can include size, wetness, porosity, and composition, as well as spatial coordinates. This vector is represented by $\mathbf{x}$. The first term in Eq. (1) is the temporal component, representing changes over time. The second term accounts for changes in each property, such as an increase in liquid volume due to liquid addition or a decrease in porosity due to consolidation. This term can also account for particle fluxes when the property is a spatial coordinate. The source terms $\Re_{formation}$ and $\Re_{depletion}$ represent the change in particles within each class from aggregation, breakage, or nucleation.

PBMs have been used to model various powder processes, such as crystallization (Gerstlauer et al., 2002), powder mixing (Sen and Ramachandran, 2013), and milling (Bilgili and Scarlett, 2005), and wet granulation (Cameron et al., 2005; Verkoeijen et al., 2002). Most PBMs found in the literature are one-dimensional; they only consider distributions with respect to one particle property, typically size. Because wet granulation is a complex process facilitated by a liquid binder, 1-D PBMs have limited accuracy in representing real processes (Iveson, 2002). As a consequence, multi-dimensional PBMs have been developed using three internal coordinates: solid, liquid, and gas volume (Poon et al., 2008). Some studies have also used multiple internal coordinates to model two solid components, which may result in inhomogeneous distributions (Matsoukas and Marshall, 2010; Matsoukas et al., 2009; Marshall et al., 2011, 2012). Although these models can simulate more complex behavior, they are more computationally expensive and require many empirical expressions and parameters (Barrasso and Ramachandran, 2012). These models may be unsuitable for iterative calculations, such as parameter estimation and optimization. Reduced order modeling has been proposed as an alternative, representing one or more particle properties as a lumped parameter within the remaining internal coordinate system to reduce the dimensionality of the problem (Barrasso and Ramachandran, 2012; Hounslow et al., 2001; Biggs et al., 2003). This technique drastically reduces the computational time, but it may result in a loss of information and fail to represent wide distributions in lumped properties (Barrasso and Ramachandran, 2012).

Additionally, spatial coordinates are not inherent in traditional PBMs. Spatial compartments can be defined to simulate inhomogeneities within the equipment. The equipment is divided into geometric regions, often related to zones of liquid addition, impeller, and chopper action. A three compartment PBM for a fluidized-bed granulator was developed by Maronga and Wnukowski (1997), dividing the granulator into spraying, drying, and inactive zones using empirical values for the rate of transfer between the domains. Similarly, a two-compartment PBM for a Wurstur fluidized bed is presented by Borner et al. (2013), based on spraying and drying zones. In horizontal, continuous operation, granules develop along the axial coordinate. A continuous wet granulator has been simulated using axial spatial compartments by Barrasso et al. (2013b). A drawback of compartmental modeling is that an additional model is required to describe the flux between neighboring compartments since the PBM cannot independently describe particle flow. Some studies have used DEM to complete the compartmental model, using flux data from DEM simulations as input data to the PBM (Sen and Ramachandran, 2013; Freireich et al., 2011; Sen et al., 2012; Li et al., 2013).

Various rate expressions are needed to describe the subprocesses of consolidation, liquid addition, breakage, and aggregation. An exponential decay function is often used to describe the consolidation rate, but this approach contains multiple empirical parameters and does not account for the effect of liquid binder content on consolidation, which has been observed experimentally (Verkoeijen et al., 2002; Iveson et al., 1996). Similarly, liquid addition rates require assumptions about the distribution of liquid to the particles. A homogeneous distribution based on particle mass or surface area is often assumed, although heterogeneity has been observed (Scott et al., 2000; Stepanek et al., 2009). Empirical and mechanistic expressions have been developed to describe the breakage rate (Pandya and Spielman, 1983; Pinto et al., 2007; Ramachandran et al., 2009) as it depends on particle properties and process parameters, but these kernels contain additional empirical parameters or particle data that is not inherently known in PBMs, such as particle shear forces.

The aggregation rate is the most investigated, with empirical and semi-empirical rate kernels describing the effect of size on the rate of aggregation. Hounslow et al. (2001) proposed a size-independent kernel (SIK), Smoluchowski's shear kernel (SSK) and the equipartition of kinetic energy kernel (EKE). Numerous alternative size-dependent kernels have also been proposed (Cameron et al., 2005). Fewer aggregation kernels describe the effect of the liquid binder content. The kernel presented by Madec et al. (2003), accounts for size and liquid content, containing three empirical parameters. Additionally, Wauters (2001) proposed a simple kernel based on size and liquid content that categorizes particles as large or small and wet or dry, defining a rate of zero or one for each combination.

Mechanistic or semi-mechanistic aggregation kernels have also been developed. Typically, the aggregation rate is broken into two multiplicative factors. The collision frequency describes the transport of particles, or the rate of collisions between each pair of particle sizes. DEM simulations have been used to analyze the collision frequency distribution by Gantt et al. (2006). The second factor, the collision efficiency, determines whether two colliding particles will aggregate based on particle sizes and surface wetness, relative velocities, and material properties. Expressions for coalescence criteria have been developed (Gantt et al., 2006; Liu and Litster, 2002; Chua et al., 2013). Both the collision frequency and efficiency require information that is unknown in PBMs, such as the collision frequency distribution, particle surface liquid, and relative velocities. DEM simulations can be useful in obtaining this information.

In order to obtain realistic values for the unknown parameters in empirical and semi-empirical rate expressions, parameter estimation has been performed using experimental data (Darelius et al., 2006; Poon et al., 2009; Braumann et al., 2010; Ramachandran and Barton, 2010). Parameter estimation has also been used with 1-D PBMs for other powder processes, such as milling (Capece et al., 2011; Barrasso et al., 2013a). When many parameters are used, substantial experimental data is required, or the model is computationally intensive, this approach is not ideal. Further, these models may not fully capture the complex nature of granulation processes. In order to reduce the number of unknown parameters and capture complex trends, a more mechanistic approach is required, such as multi-scale modeling using DEM.

2.2. *Discrete element modeling*

In contrast to the PBM, DEM simulations track each particle as it moves through space, collides with equipment and other particles, and is subject to force fields, such as gravity. These models primarily use Newton's laws of motion, expressed in Eqs. (2) and (3) (Cameron et al., 2005).

$$m_i \frac{dv_i}{dt} = F_{i,net} \tag{2}$$

$$F_{i,net} = F_{i,coll} + F_{i,ext} \tag{3}$$

In these equations, the mass of particle i is given by m_i, and the velocity is given by v_i. $F_{i,net}$ is the net force acting on the particle, which is the some of the forces due to collisions ($F_{i,coll}$) and the external forces ($F_{i,ext}$), such as gravity. When coupled with Navier–Stokes equations or computational fluid dynamics (CFD), fluid–particle forces are also included. Various contact models can be implemented to describe the collision behavior, such as the hard-sphere model, the Hertz–Mindlin model, and the Johnson–Kendall–Roberts (JKR) model. The non-linear elastic Hertz–Mindlin contact model is used in this study.

Commercial DEM software is available, such as EDEM (DEM Solutions), which contain graphical user interfaces for easy use. However, DEM is highly computationally intensive, with single simulations taking hours or days to solve. Parallel computing can be used to reduce computation time (DEM Solutions, 2013). DEM is not suitable for iterative calculations, such as parameter estimation or optimization. Furthermore, the number of particles is a limiting factor, and many DEM simulations contain a drastically reduced number of particles compared to those observed in real systems, often with larger particles used to represent a fixed number of smaller particles (Hassanpour et al., 2009). Collision detection is the limiting calculation in DEM, and smaller particles require a finer grid to perform this operation (DEM Solutions, 2013). Periodic sectioning can also be used to reduce the number of particles in a simulation (Gao et al., 2011).

Microscale DEM simulations involve fewer particles in order to obtain mechanistic results. Lian et al. (1998) simulated two-particle interactions and impact coalescence between wet agglomerates using DEM, and Kafui and Thornton (2000) performed simulations of impact breakage. While these studies provide micro-scale insight into granulation mechanisms,

they are not directly applicable to process-level simulations. Gantt et al. (2006) studied the interactions of 5000 particles with a mean size of 1.7 mm within a periodic boundary and extracted data to provide statistical estimates of coalescence rates and efficiencies. These results can help connect mechanistic, micro-scale modeling with process-level models, such as the population balance. However, these simulations do not incorporate the rate processes observed in granulation, but can serve as input data for a PBM. The effects of size distribution, segregation, liquid distribution, and process parameters are not captured by this approach. At the process level, DEM simulations for powder flow and mixing have also been used to generate reduced order models for use in flowsheet simulations by Boukouvala et al. (2013). A similar approach can be used to overcome the computational limitations of DEM within process-level simulations.

2.3. Comparison of PBM and DEM

While the PBM framework is largely empirical, DEM simulates particle-scale behavior. DEM inherently determines spatial effects, such as segregation and particle flux. Additionally, liquid binder droplet distribution has been simulated using DEM, representing binder droplets as solid particles that can merge with powder particles on contact (Goldschmidt et al., 2003). Further, each collision is treated as a separate event, and collision properties such as frequency, relative velocity, and particle properties can be extracted from the results for use in mechanistic kernels.

A critical difference between PBM and DEM is the treatment of the rate processes. DEM must be coupled with an additional model to simulate rate processes such as aggregation, consolidation, and breakage. Previously, aggregation has been represented by cohesion of spherical particles on contact, which result in agglomerates of spheres (Tardos et al., 1997). This approach is computationally intensive but provides insight into granule morphology. Alternatively, particles that coalesce can be replaced with a larger spherical particle by applying a conservation of mass (Goldschmidt et al., 2003). In this sense, DEM is used as a simulation tool for solving a PBM. Both approaches require the aggregation criteria to be defined.

Some recent studies involve coupling of a PBM with DEM. In a study by Reinhold and Briesen (2012), DEM is coupled concurrently to a 1-D PBM to account for aggregation. Similarly, Dosta et al. (2013) performed multiscale modeling of a granulation process using a 1-D PBM to generate size distributions and DEM to simulate particle-scale behavior. Additionally, Wang et al. (2012) simulated a ball milling process using DEM to obtain collision and dissipation energies, which were used in a PBM to simulate breakage.

Coupling DEM with other modeling tools is a subject of interest. Many models have been developed using DEM coupled with CFD for particle–fluid interaction in fluidized-bed granulation processes (Fries et al., 2011, 2013; Jajcevic et al., 2013). However, fewer studies integrate PBM and DEM simulations. One-way coupling has been used to incorporate powder flow data into compartmental PBMs for various powder processes (Sen and Ramachandran, 2013; Freireich et al., 2011; Sen et al., 2012; Li et al., 2013). Other models use DEM-generated coalescence kernels within a PBM (Liu and Litster, 2002; Gantt and Gatzke, 2006). With drastic particle size changes, as found in granulation, a two-way coupling approach may provide additional data as the particle size distribution (PSD) can effect large-scale behavior.

The two approaches for representing size enlargement due to aggregation within a DEM simulation have been presented, effectively solving the PBM using DEM (Goldschmidt et al., 2003; Tardos et al., 1997). A third approach is presented here, collecting collision and particle data from a DEM simulation over a specified time interval and applying a PBM to update the size distribution within the DEM. This two-way coupling approach requires collisions to be counted and stored, but does not require immediate action, reducing the computational expense of each collision. Additionally, the dynamic DEM data can be used to generate a reduced order model, replacing the expensive DEM step.

3. Model development

3.1. Population balance model

A two-dimensional PBM was used to track the PSD over time during granulation, using solid and liquid volume as internal coordinates. The general form of this equation is given by

$$\frac{\partial}{\partial t}F(s,l,t)+\frac{\partial}{\partial l}\left[F(s,l,t)\frac{dl}{dt}\right]=\Re_{agg}(s,l,t), \tag{4}$$

where s and l represent the volumes of solid and liquid per particle, respectively. This equation includes the rate processes of liquid addition (represented by the partial derivative with respect to l) and aggregation ($\Re_{agg}$). In the hybrid model, liquid addition is simulated using DEM, so it must be omitted from the PBM. The PBM becomes

$$\frac{\partial}{\partial t}F(s,l,t)=\Re_{agg}(s,l,t). \tag{5}$$

The net aggregation rate consists of the depletion of smaller particles as they aggregate ($\Re_{agg,form}$) and the formation of larger granules ($\Re_{agg,dep}$), as shown in Eq. (6).

$$\Re_{agg}(s,l,t)=\Re_{agg,form}(s,l,t)-\Re_{agg,dep}(s,l,t) \tag{6}$$

The expressions for these rates are given in Eqs. (7) and (8).

$$\Re_{agg,form}(s,l,t)=\frac{1}{2}\int_0^s\int_0^l\beta(s-s',l-l',s',l',t)\,F(s-s',l-l',t)F(s',l',t)\,dl'\,ds' \tag{7}$$

$$\Re_{agg,dep}(s,l,t)=\int_0^\infty\int_0^\infty\beta(s,l,s',l',t)F(s',l',t)F(s,l,t)\,dl'\,ds' \tag{8}$$

Here, $\beta(s,l,s',l',t)$ is the aggregation kernel, describing the rate of aggregation as it depends on the properties of the two colliding particles and time. The aggregation kernel can be broken into two factors: the collision frequency, C, and the collision efficiency, Ψ, shown in Eq. (9).

$$\beta(s,l,s',l',t)=C(s,l,s',l',t)\Psi(s,l,s',l') \tag{9}$$

The collision frequency describes the rate of collision between particles as a function of particle properties. It has

previously been demonstrated using DEM that particle size affects the collision frequency (Gantt et al., 2006).

The time dependency of the collision frequency is included to account for the effects of the current state of the system on the aggregation rate. For example, the PSD may affect the collision frequency. To test this hypothesis, DEM simulations were performed using different PSDs, and the collision frequency was calculated. The results of this investigation are presented in this study, confirming the effect of PSD on the collision frequency.

In the hybrid model, all collisions are recorded using DEM to calculate the collision frequency in real time. Based on the total number of collisions between each particle N_{coll} during the time interval Δt, the collision frequency can be determined from Eq. (10), which normalizes the collision rate by the number of particles (Gantt et al., 2006).

$$C(s, l, s', l', t) = \frac{N_{coll}(s, l, s', l', t)}{F(s, l, t)F(s', l', t)\,\Delta t} \tag{10}$$

The collision efficiency describes the likelihood that two colliding particles will aggregate. Coalescence is determine by particle properties, such as size, surface liquid, and porosity, as well as collision properties, such as relative velocity (Gantt et al., 2006). Mechanistic expressions have been developed to assess whether collisions will occur using particle-scale models. DEM simulations can be used to assess the collision properties and develop empirical expressions for the collision efficiency (Gantt et al., 2006). However, the effects of process parameters and material properties on the collision behavior is unknown.

In this study, a simple expression for the collision efficiency is used, as shown in Eq. (11), adapted from Biggs et al. (2003).

$$\Psi(s, l, s', l') = \begin{cases} \Psi_0 & LC(s, l) \geq LC_{\min} \text{ or } LC(s', l') \geq LC_{\min} \\ 0 & LC(s, l) < LC_{\min} \text{ and } LC(s', l') < LC_{\min} \end{cases} \tag{11}$$

Here, LC is the particle liquid content, given by $LC(s, l) = l/(s + l)$, and LC_{min} is the minimum liquid content required for coalescence. This expression states that if either of the colliding particles have a liquid content greater than a minimum value, coalescence can occur upon collision. Ψ_0 is a rate constant defining the probability of coalescence for all collisions that meet the liquid content criterion. The values for LC_{min} and Ψ_0 are given in Table 1. Future work will involve coupling the DEM results to the PBM to determine the collision efficiency in addition to the frequency.

3.2. Discrete element model

Simulations were performed using EDEM 2.5 Academic Simulator (DEM Solutions) on an Intel Core i7-2600 CPU processor (3.4 GHz) with 16 GB of RAM. A User Defined Library (UDL) was created using C++ to implement the PBM and custom liquid addition model within the simulation. The UDL was written to enable multi-threading, and the simulations were performed with 4 cores.

A batch drum granulator was selected for its simple geometry (Poon et al., 2009). The equipment was modeled as a horizontal cylinder, and the dimensions and rotational speed are listed in Table 1. Four baffles were created as thin, flat plates along the granulator wall to agitate the particles. The model can be extended to simulate more complex equipment, such as those with impellers or screws (high-shear, twin-screw), as well as those with spatial inhomogeneities.

Table 1 – Parameters and initial conditions for simulation. Values for parameters used in DEM simulations* were taken from Dubey et al. (2011).

Parameter	Value
Solid volume of first bin, s(1)	0.5 mm^3
Liquid volume of first bin, l(1)	0.5 mm^3
Initial number of powder particles	15,000
Initial powder particle bin	[1,0]
Initial liquid droplet bin	[0, 1]
Simulation time, t_{sim}	10 s
PBM time interval size, Δt	0.01 s, 0.1 s, 1 s
DEM time step	1×10^{-5} s
DEM grid size	2 mm
Liquid addition start time	0.1 s
Liquid addition end time	5.1 s
Total liquid-to-solid ratio, L/S	0.33
Drum diameter, D	40 mm
Drum length, L	60 mm
Baffle width	4 mm
Number of baffles	4
Drum rotational speed	60 RPM
Collision efficiency constant, Ψ_0	0.001
Minimum liquid content for coalescence, LC_{min}	0.15
Poisson's ratio*	0.25
Shear modulus*	2 MPa
Particle density	1 g/cm^3
Coefficient of restitution*	0.1
Coefficient of static friction*	0.5
Coefficient of rolling friction*	0.01

Primary powder particles were defined to have a uniform volume of 0.5 mm^3 or approximately 1 mm in diameter. This size is much larger than the primary particles used in real granulation processes, in order to fill an acceptable fraction of the drum with 15,000 particles. Particle scaling is typical in DEM simulations, which have computational limitations. A greater number of particles increases the computational burden on DEM, and smaller particles require a smaller time step for contact detection. The particles are initially placed randomly throughout the drum and settle at the bottom before the start of liquid addition. Additional particle properties are listed in Table 1. Several properties relevant to the DEM simulation were selected from Dubey et al. (2011), and experimental studies are needed to fully characterize these material properties.

Liquid droplets were modeled as solid particles with the same properties as the primary powder particles. A cylindrical region of 8 mm in diameter was created as the liquid addition zone. This region spanned the length of the granulator and is centered 8 mm below the top of the granulator to prevent liquid creation in the baffle region. Liquid particles were created during the time interval of 0.1–5.1 s, allowing the powder particles to settle before liquid addition begins. This time period is known as the liquid addition period of the granulation process. The wet massing period occurs after liquid addition ends, from 5.1 s to 10 s. An overall liquid-to-solid ratio of 1/3 was used, and liquid particles were created at a rate of 1000 s^{-1}. Upon contact with a powder particle, the liquid droplet disappears, and the liquid volume of the powder particle increases. This event changes the liquid bin of the particle, eliminating the need to simulate liquid addition within the PBM. If a liquid particle collides with another liquid particle, they merge to create a larger droplet. Using DEM to simulate liquid addition allows for inhomogeneities

in liquid distribution, an effect that is not inherent in the PBM.

Powder–powder and powder–wall collisions were simulated using the Hertz–Mindlin model as provided by EDEM. The Hertz–Mindlin model is a non-linear, elastic model that calculates the normal and tangential contact forces on each body. The governing equations of this model are presented in Appendix A. This contact model was selected for its simplicity, but other non-cohesive contact models can be used within this hybrid model framework. Liquid-particle collisions, which resulted in immediate coalescence, were simulated to apply no contact force on the new particle.

All particle–particle collisions were recorded and counted according to the sizes of the colliding particles. A four-dimensional array containing the total number of collisions between particles in each solid and liquid bin was generated and used within the PBM. The collision count was reset to zero after each PBM iteration.

The simulations were run for a total time of 10 s, with a fixed DEM time step of 1×10^{-5} s. The geometric grid was simulated using a cell size of 2 mm.

3.3. *Two-way coupling*

A multi-scale model was created in which the PBM and DEM transfer information during the simulation. A schematic of this approach is shown in Fig. 1.

The PBM is used in the hybrid model to calculate the change in the number of particles of each solid and liquid volume over a set time interval. A linear grid with respect to volume was implemented. The initial particles were defined to be perfectly dry ($l = 0$), with a uniform initial solid volume, shown in Table 1, and liquid droplets contained no solid ($s = 0$), and had a uniform initial liquid volume. The initial volumes were used to space the bins equally along a grid. The fully discretized form of this model is given by Eq. (12), which uses Euler integration to determine the change in the number of particles, ΔF, over the time interval.

$$\begin{aligned}\Delta F(s,l,t) = &\sum_{s'=0}^{s}\sum_{l'=0}^{l} N_{coll}(s-s',l-l',s',l',t)\Psi(s-s',l-l',s',l') \\ &- \sum_{s'=0}^{s_{max}-sl_{max}-l}\sum_{l'=0} N_{coll}(s,l,s',l',t)\Psi(s,l,s',l') \\ &- \sum_{s'=0}^{s_{max}-sl_{max}-l}\sum_{l'=0} N_{coll}(s',l',s,l,t)\Psi(s',l',s,l) \end{aligned} \quad (12)$$

s_{max} and l_{max} are the maximum solid and liquid volumes found in a particle within the DEM simulation, which can change over time. These summations take advantage of the discrete nature of DEM, only performing calculations on particles that exist within the simulation. This approach circumvents the computational limitations of the grid size, as the maximum number of populated bins is a finite number less than the initial number of particles.

The number of collisions between each pair of bins over the time interval is recorded within the DEM simulation and transferred to the PBM. It should be noted that the number of particles in each bin, the normalized collision frequency, and the time interval size are not required to solve Eq. (12) because they cancel out when combining Eqs. (7)–(10).

Each time the PBM is solved, a change in the particle distribution is calculated. To implement this change in DEM, particles are immediately destroyed or created. When ΔF is negative for a particular bin, particles must be destroyed. Particles within that bin are randomly selected and removed from the simulation.

Creating particles is more complex. When ΔF is positive, particles are created with the properties defined by the bin. A random position is assigned to the particle. Before creation, the new particle's position and size are checked against all other particles in the simulation to determine if there is overlap. A new position is attempted until the new particle

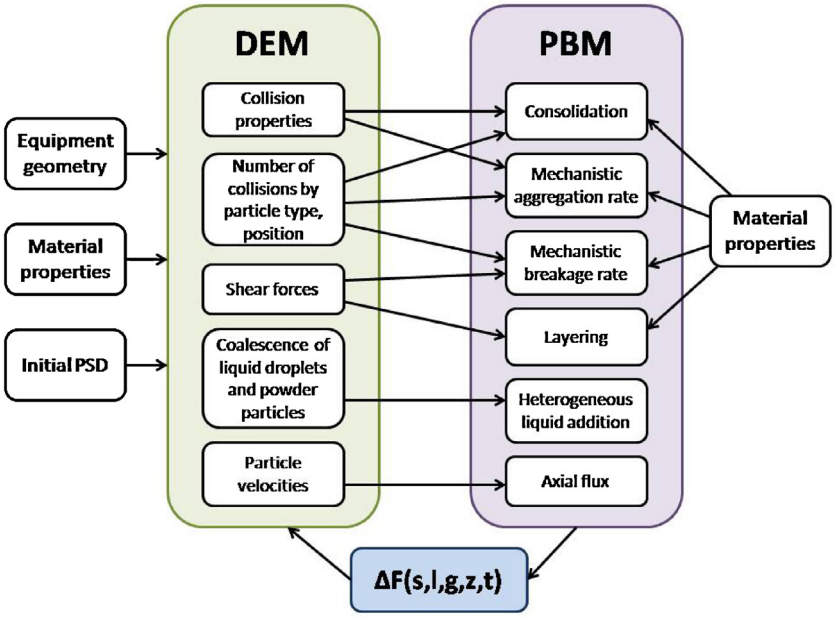

Fig. 1 – Schematic of multi-scale model and data transfer. In this study, the collision frequency and liquid addition behavior are considered to demonstrate the coupling algorithm. Remaining features will be presented in future work.

does not overlap with any existing particles. This calculation requires the storage of each particle position and size at every step of the PBM. However, because the PBM is much less computationally demanding than the DEM, the effect on the total computation time is negligible. In simulations with a much greater number of particles or less available space, this computation may be inefficient.

Because DEM requires a discrete number of particles, fractional values of ΔF cannot be implemented. If the number of coalescence events between two bins, given by $N_{coll}\Psi$, is not a whole number, it must be rounded. A random number between zero and one is generated and compared to the decimal component of $N_{coll}\Psi$ to determine whether to round the number up or down to the nearest integer. While this rounding may have a small effect on the results, it is more representative of the discrete granulation process, where fractions of particles cannot exist.

The PBM is evaluated at specified time intervals, given by Δt. The time interval size was selected such that the randomly placed particles have ample time to settle and collide between PBM evaluations, minimizing the effect of their placement. Additionally, the time interval size must be small enough that the number of coalescing particles in a given bin is not greater than the number of existing particles. If each particle collides many times over a time interval, more than one coalescence event per particle may result. This requirement is an example of the Courant–Friedrichs–Lewy (CFL) condition, given by Eq. (13)

$$\frac{u \times \Delta t}{\Delta x} = C < 1, \tag{13}$$

where u is the velocity or growth rate, Δx is the grid spacing, and C is the Courant number (Ramachandran and Barton, 2010). Since this PBM does not include a growth rate, but instead includes a source term for the aggregation rate, the CFL condition can be adapted to form Eq. (14).

$$-\frac{\Re_{agg} \times \Delta t}{F} = C < 1 \tag{14}$$

Three PBM time intervals were used to investigate these effects, as given in Table 1. A replicate simulation was performed with a PBM time interval of 0.1 s to demonstrate reproducibility and variation in the results due to random particle placement at the beginning and during the simulation.

4. Results and discussion

4.1. *Effect of particle size distribution on collision rates*

It has been reported that the collision rate is a function of particle size, and as a consequence various rate kernels have been proposed to capture this effect (Gantt et al., 2006; Tan et al., 2004; Darelius et al., 2005). However, no studies have captured the effect of the PSD on the collision frequency. Since the collision frequency is related to the packing of the particles and the interstitial space between large particles, the size distribution will affect the collision rate and its dependence on particle size. As the size distribution changes over time within the granulator, the collision frequency will also change, accounting for the temporal component of the aggregation kernel, which traditionally has been lumped as an empirical constant that needs to be fitted from experimental data, thus limiting the predictive capability of the model.

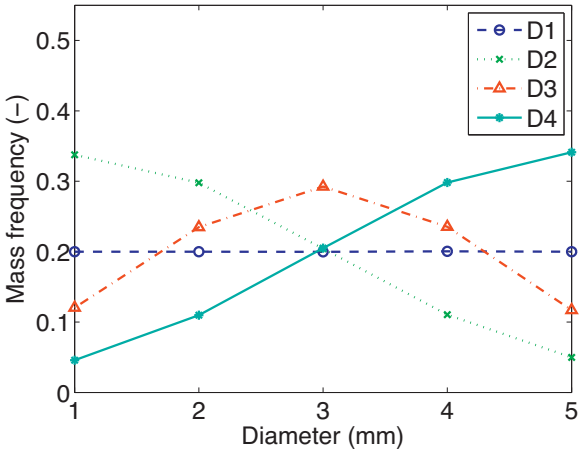

Fig. 2 – Size distributions used in DEM simulations to determine collision rates, from 1 to 5 mm in diameter.

To demonstrate the effect of the size distribution on the collision rate, DEM simulations were performed using four distributions, as presented in Fig. 2. The collision rate, as a function of particle size, was determined independently for each distribution. Five particle types were defined with diameters between 1 mm and 5 mm. The number of particles of each size was varied to match the four distributions. The rotating drum granulator was filled with particles equaling a total volume 7500 mm^3 according to the distributions presented. The particles were allowed to settle for 0.5 s. The number of collisions between each particle size during the 0.5–1.5 s interval was recorded. These totals were converted into normalized collision rates according to Eq. (10). No size changes were implemented during these simulations.

The collision rates for each distribution are shown in Fig. 3. In all cases, larger particles had greater collision rates than smaller particles. Small particles had lower collision rates with other small particles than with larger particles. Particles of similar sizes were collided with each other less frequently than with particles of slightly different sizes, shown by the drop in collision rates along the axis of symmetry.

Despite these similarities, measurable differences are observed. The uniform size distribution (D1) showed similar trends as the size distribution with a greater frequency of medium-sized particles (D3). These distributions were the most similar, with the same median diameter. However, D3 shows lower collision frequencies between the largest particles and greater collision frequencies between medium-sized particles with large and small particles.

The skewed distributions showed greater differences. The distribution with a greater frequency of small particles (D2) showed lower collision frequencies overall, and the distribution with a greater frequency of large particles (D4) had greater collision frequencies. D2 shows strong size dependence, with larger particles colliding much more frequently than smaller particles. D4 showed a weaker size dependence, with large particles colliding with small particles most frequently, and particles of similar sizes colliding less often.

As the PSD develops within a granulator, the collision dynamics will also change. A PBM typically assumes that every particle can collide with every other particle, often at equal rates. Aggregation kernels can be used to account for the effects of size and other particle properties on the collision

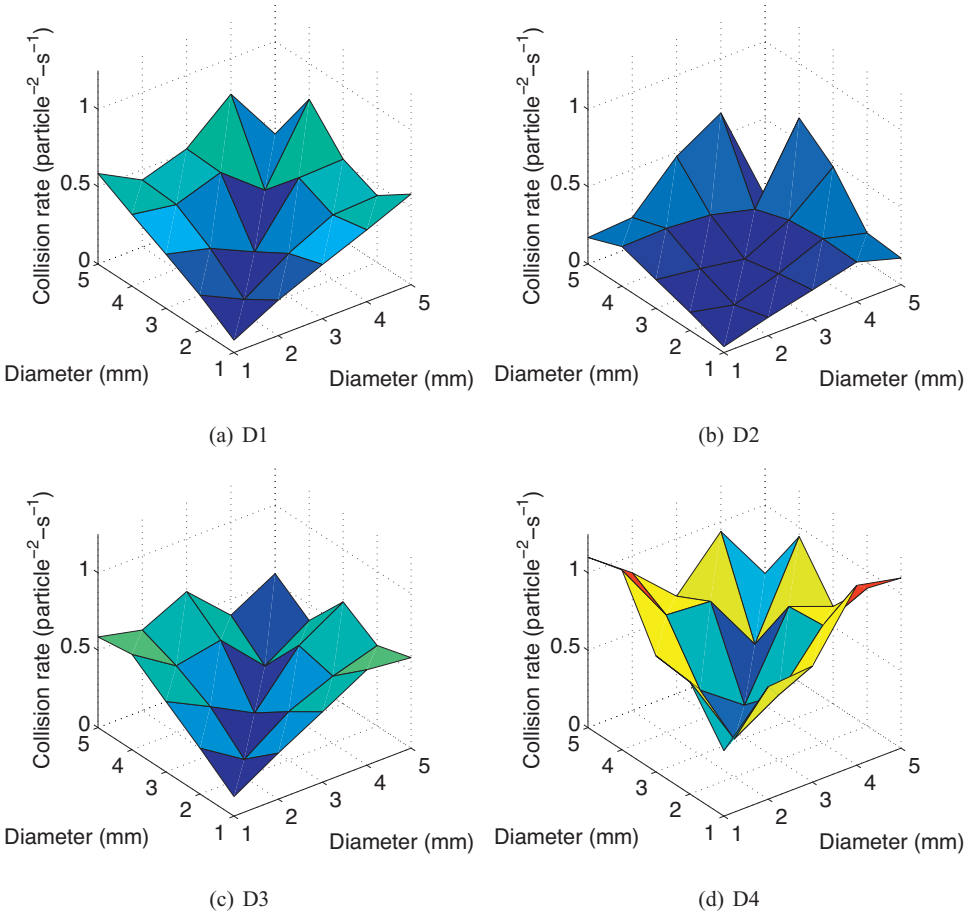

Fig. 3 – Collision frequency versus particle size for each distribution based on DEM simulations.

frequency and efficiency. However, no kernels describe the effects of the current size distribution on the aggregation rate. The effect of size on the collision frequency is dependent on the size distribution, and this interaction cannot be captured with a simple, size-dependent kernel. Because the collision frequency affects the aggregation rate, the temporal change in the size distribution is affected by the collision rate and, by extension, the current distribution.

To simulate this behavior within a process model, the collision rates must be updated in real time as the PBM is solved, demonstrating the need for bi-directional coupling of PBM with DEM. Because of the high computational expense of DEM, future approaches may involve developing a reduced order model to determine the effects of particle size and size distribution on the collision frequency.

4.2. *Hybrid model results*

The fully-coupled hybrid model was used to simulate a simple rotating drum cylinder for a 10-s period. The simulation was completed in approximately 6 h.

Fig. 4 shows the conservation of solid and liquid volume over time. The total solid volume is constant over time, and the total liquid volume increases linearly during the liquid addition period but remains constant at all other times. These results support the validity of the numerical techniques used to solve the PBM and confirm the accuracy in implementing particle changes within the DEM.

Fig. 5 shows the particles within the granulator at four different times, colored according to their liquid fraction for the simulation with a PBM time interval of 0.01 s. Large particles develop over time as the particles aggregate. The largest particle present in the system at 5 s has a diameter of 2.76 mm and a liquid fraction of 0.36, corresponding to the PBM bin of [21,12]. At 10 s, the largest particle has a diameter of 4.64 mm and a liquid fraction of 0.30, corresponding to the PBM bin of [100,42].

The greatest liquid fraction of a powder particle decreases over time during the wet-massing period as aggregation occurs and wet particles merge with dryer particles. The greatest liquid fraction at 5 s is 0.75 for a particle of 1.44 mm in diameter. At 10 s, the greatest liquid fraction is 0.59 for a particle of 2.08 mm in diameter.

The average particle diameter increases from 0.98 mm to about 2.5 mm during the liquid addition and wet massing periods, as shown in Fig. 6. This plot shows a discontinuous increase in average diameter for the simulation with the PBM time interval of 1 s, which can be attributed to the low frequency of PBM solution and particle replacement. Despite this result, all simulations resulted in approximately the same average diameter, presented in Table 2. The final $d_{4,3}$ of with a PBM time interval of 0.1 s were approximately 2.5% different than that of the PBM time interval of 0.01 s, suggesting that a PBM time interval of 0.1 s is sufficient to solve this model. The replicate simulations with a PBM time interval of 0.1 s resulted in slightly different average diameters, indicating some effect of the random placement of particles.

The average liquid fraction of each size class is shown in Fig. 7. The average liquid fraction of the smallest particles

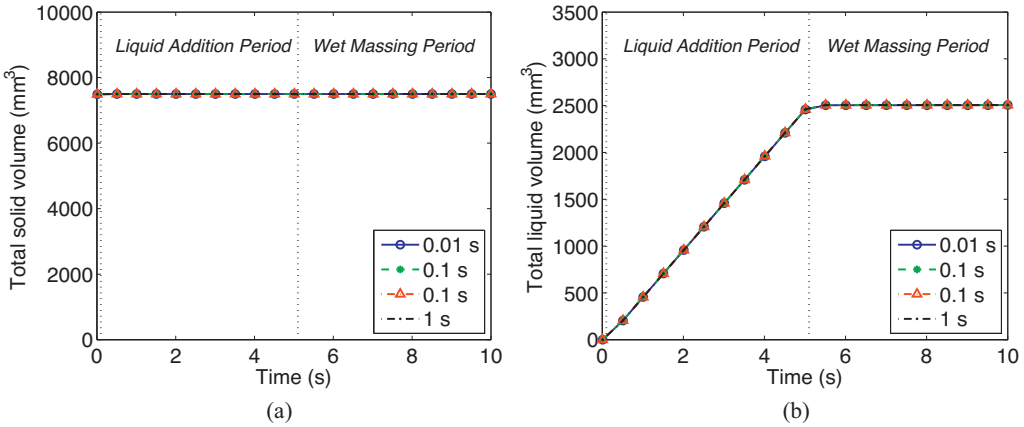

Fig. 4 – Total volumes of (a) solid and (b) liquid in the system over time for simulations of varying PBM time intervals. Replicate simulation performed at time interval of 0.1 s to show reproducibility.

increases during the liquid addition period, but decreases during the wet massing period as the wet particles aggregate and move to larger size classes. As particles form in each size class, the average liquid fractions of the larger size classes are high, a result of the wet particles aggregating. These values decrease over time as the large, wet particles aggregate with small, dry particles, reducing the average liquid content of the size class.

Table 2 – Average diameter ($d_{4,3}$) after 10 s for simulations of varying PBM time intervals and percent error based on results of 0.01 s PBM time interval.

PBM time interval (s)	$d_{4,3}$ (mm)	Percent error
0.01	2.525	–
0.1	2.523	0.11
0.1	2.461	2.55
1	2.47	2.26

Fig. 8 shows the PSDs at the end of each simulation. These distributions show that the simulation with the largest PBM time interval has a higher peak, or a lower frequency of very large and very small particles. This result can be attributed to numerical error. The PBM was only solved ten times in this simulation, limiting the opportunities for large particles to collide and aggregate with each other. The distributions for the smaller time intervals show more consistent results, suggesting that they are approaching an accurate solution.

The PSDs over time, presented in Fig. 9, show a progression toward larger particles during granulation. An initially narrow size distribution widens over time to include larger particles. The mass frequency of smaller particles decreases,

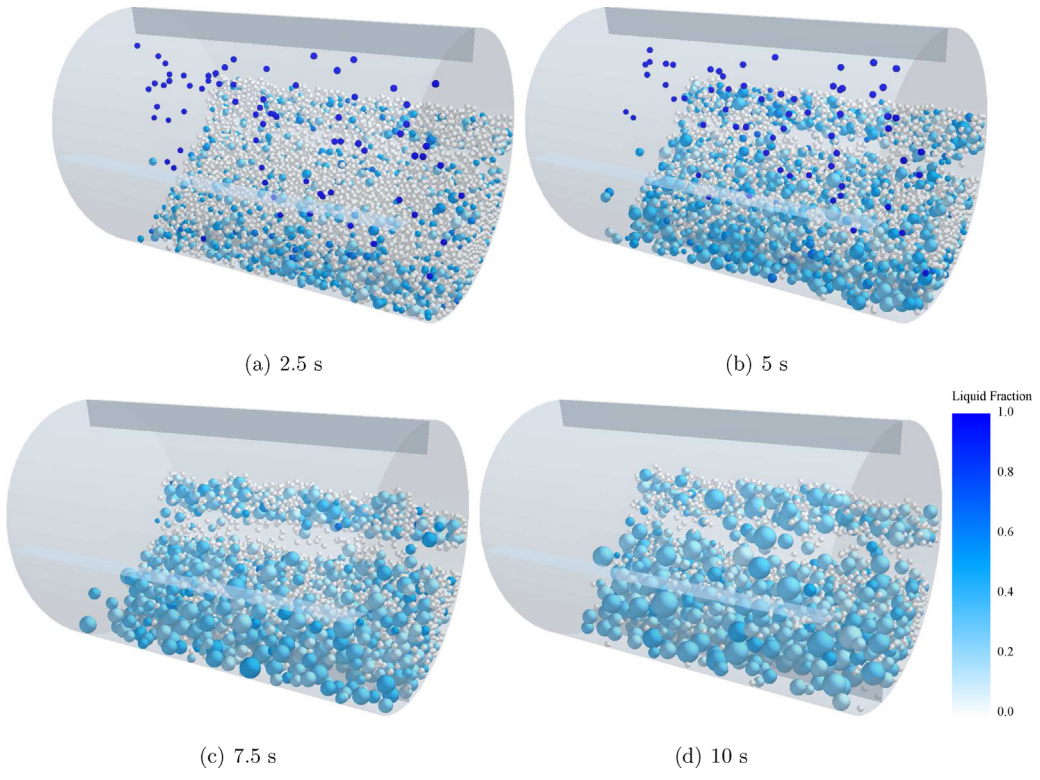

Fig. 5 – DEM image of particles at various times, colored by liquid fraction, using a PBM time interval of 0.01 s.

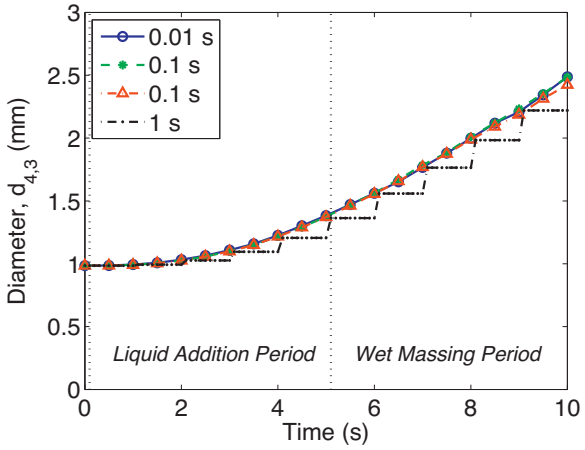

Fig. 6 – Average diameter ($d_{4,3}$) over time of the powder particles for simulations of varying PBM time intervals. Replicate simulation performed at time interval of 0.1 s to show reproducibility.

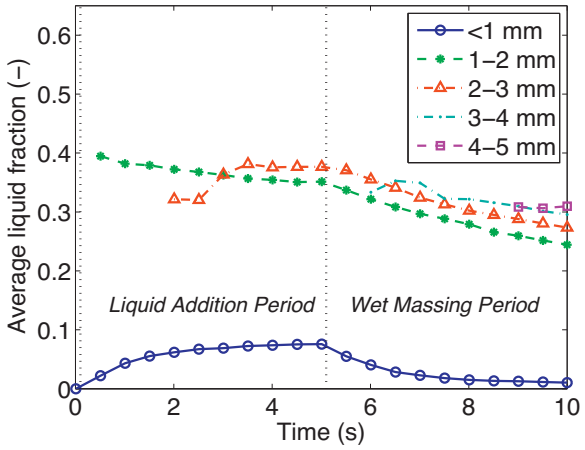

Fig. 7 – Average liquid fraction of powder particles over time for each size class, weighted by volume, for coupling time of 0.01 s.

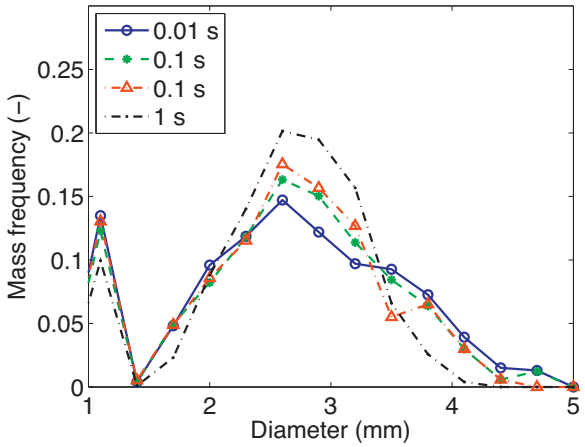

Fig. 8 – PSDs after 10 s for simulations of varying PBM time intervals. Replicate simulation performed at time interval of 0.1 s to show reproducibility.

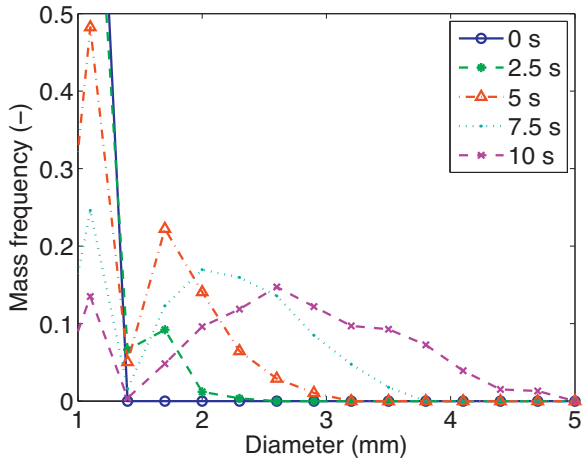

Fig. 9 – PSDs at various times using a PBM time interval of 0.01 s.

but many of the small particles still exist after 10 s. This observation can be attributed to the inhomogeneous distribution of liquid, leaving many particles dry and unable to aggregate unless they collide with wet particles.

Two-dimensional particle distributions in size and liquid content support this explanation, as shown in Fig. 10. The results show that even after 10 s, the remaining small particles are completely dry. Additionally, during the liquid addition period, small, wet particles are present, but during the wet massing period, the only wet particles in the system are much larger. These results are consistent with the liquid-dependent collision efficiency used in the PBM.

The trends observed in this study are qualitatively consistent with experimental results. Experimental PSDs presented by Poon et al. (2009) are bimodal, with a shrinking frequency of primary particles over time and an increasing number of large particles. Ramachandran et al. (2008) also show bimodal PSDs that broaden over time, along with variations in the liquid binder content of different size classes. Additionally, the liquid addition and wet massing dynamics observed by Pandey et al. (2013) agreed with the simulated results.

A more mechanistic expression for the collision efficiency, along with additional information transferred from the DEM, can be implemented within this framework. Future work is also needed to improve the liquid distribution model, accounting for the different sizes and properties of liquid droplets and the spatial inhomogeneities that persist during aggregation.

To simulate industrial systems, which are typically larger than those presented here, and finer particle sizes, which can be as small as 10 μm, many more particles must be simulated. The model will become more computationally expensive. The coded model can be optimized for better performance and simulated on a more advanced computer architecture to facilitate larger-scale simulations. Alternatively, reduced order models, such as artificial neural networks, can be developed and trained using DEM data to replace the computationally expensive DEM. This approach still requires a limited number of DEM simulations for training, but can result in a much faster model suitable for iterative calculations and flowsheet modeling. Current research has involved developing reduced order models in place of DEM to couple with PBM (Barrasso et al., 2014).

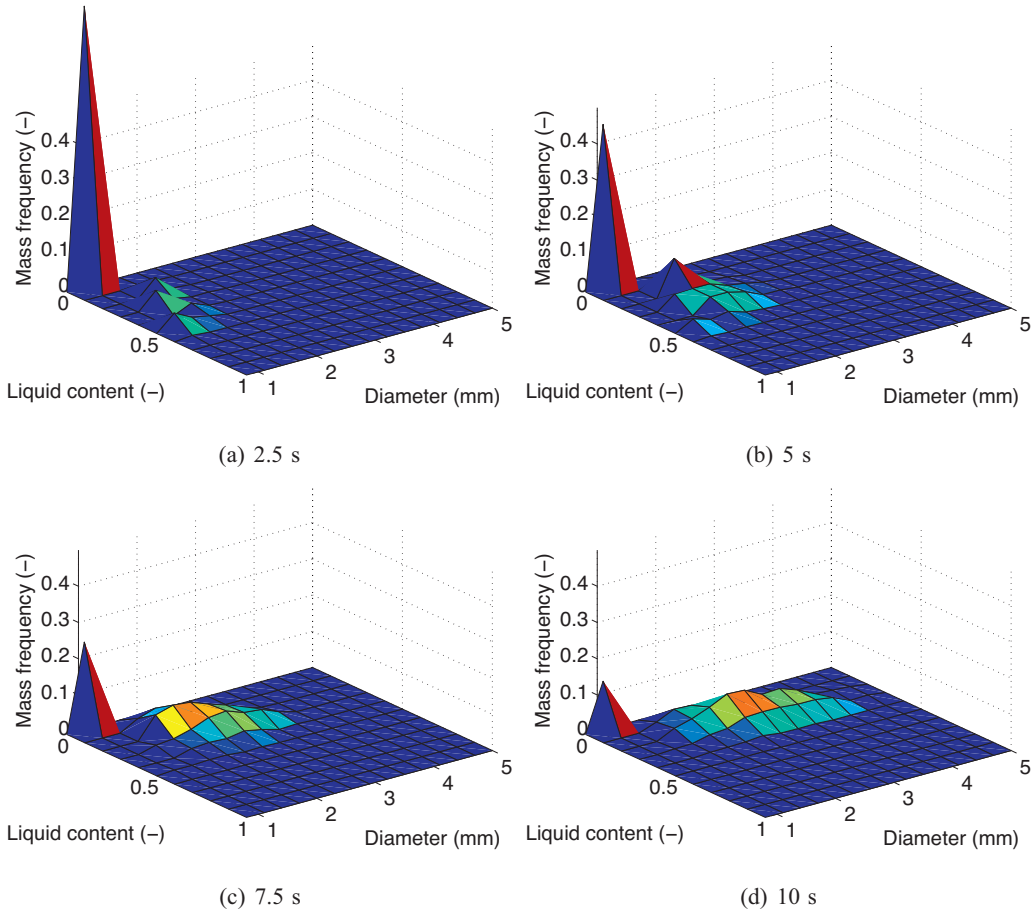

Fig. 10 – 2-D distributions of particle size and liquid content at various times using PBM time interval of 0.01 s.

5. Conclusions

In this study, a multi-scale model for wet granulation processes was presented using DEM and PBM techniques. Because PBMs rely on rate expressions, lumping all members of each class together, they have limited ability to capture the mechanistic behavior of particles in complex wet granulation processes. DEM can simulate dynamic particle-level behavior, tracking each individual particle and collision. However, DEM does not inherently simulate the sub-processes of granulation, such as aggregation and breakage. By coupling these models in real time, a hybrid modeling framework was developed.

The collision frequency between particles of different sizes was investigated. While the collision frequency is known to be dependent on particle size, the effect of the PSD had not been studied. It was demonstrated that the PSD significantly affects the shape and magnitude of the collision frequency function, accounting for the temporal dependence of the aggregation rate kernel. The collision frequency affects the aggregation rate kernel and influences the evolution of the PSD, demonstrating the need for bi-directional coupling between DEM and PBM.

A 2-D PBM was implemented within a DEM, accounting for simultaneous variations in particle size and liquid fraction. Initial particles were defined as powder or liquid, and liquid addition was handled within DEM, allowing for inhomogeneities in liquid distribution. Collision rates were recorded according to particle size and wetness, and this information was provided to the PBM at specified time intervals. The PBM calculated net changes in the number of particles, which were implemented in DEM by creating and removing particles.

The multi-scale model was successful in simulating particle size enlargement over time resulting from liquid addition and aggregation. PSDs were determined, along with 2-D distributions in size and liquid fraction. Additionally, volume conservation was demonstrated, validating the numerical techniques of the model.

An empirical expression for the collision efficiency was used in this study. The collision efficiency has been shown to depend on the relative velocity of the colliding particles, their masses, and the surface liquid available on the particles. Within this multi-scale framework, these properties can be tracked and incorporated into a mechanistic expression for the collision efficiency. Additional particle properties, such as porosity and surface/internal liquid must be included, resulting in variable density and coefficient of restitution among the particles.

Liquid droplet distribution was simulated in this study, resulting in dry fine powder and wetter large particles. The current multi-scale model simulates processes in which the liquid droplets are of comparable size to the powder particles, as is observed in sprayers, and each liquid droplet only wets one particle. In some processes, a larger droplet can wet numerous particles, often resulting in nucleation. Additional work is needed to incorporate nucleation into the existing framework. Spatial coordinates or compartments can also be included within the PBM to ensure that changes in the number of particles are implemented in the region where the rate processes are occurring.

The additional rate processes of breakage and consolidation are typically modeled using empirical expressions in PBM. However, both of these sub-processes are affected by

particle–particle and particle–wall collisions, and more mechanistic expressions can be developed using information from DEM simulations. The breakage rate depends on the forces exerted on each particle, information that is available from DEM. The consolidation rate also depends on impact forces. As particles collide with each other or equipment, they consolidate, resulting in a reduced porosity and an increased density.

Using the multi-scale framework, predictive models of wet granulation processes can be created, leading to a better understanding of the effects of material properties and process parameters on critical quality attributes. This detailed, model-based approach is necessary to accurately represent wet granulation processes and implement QbD in design, control, and optimization of powder processes.

Acknowledgements

This work is supported by the National Science Foundation Engineering Research Center on Structured Organic Particulate Systems Grant NSF-ECC 0540855. The authors also acknowledge Atul Dubey of Tridiagonal Solutions for his assistance. This work was presented and benefited from discussions at "PBM2013."

Appendix A. Hertz–Mindlin contact model

The Hertz–Mindlin contact model was used to calculate the normal and tangential forces on particles during collisions. This model was provided as a standard contact model in EDEM. The governing equations for the normal and tangential forces, F_n and F_t, resulting from a collision are given in Eqs. (A.1) and (A.2), respectively (DEM Solutions, 2013).

$$F_n = \frac{4}{3}E^*\sqrt{R^*}\delta_n^{3/2} - 2\sqrt{\frac{5}{6}}\beta\sqrt{S_n m^*}v_n^{rel} \tag{A.1}$$

$$F_t = \min\left[\mu_s F_n, -S_t\delta_t - 2\sqrt{\frac{5}{6}}\beta\sqrt{S_t m^*}v_t^{rel}\right] \tag{A.2}$$

The equivalent Young's and shear moduli are given by E^* and G^*, respectively, and R^* and m^* are the equivalent radius and mass. δ represents the overlap in the normal or tangential direction, and v^{rel} is the relative velocity. The coefficient of static friction is given by μ_s. S_n and S_t are the normal and tangential stiffness, given by Eqs. (A.3) and (A.4).

$$S_n = 2E^*\sqrt{R^*\delta_n} \tag{A.3}$$

$$S_t = 8G^*\sqrt{R^*\delta_n} \tag{A.4}$$

Finally, β is a function of the coefficient of restitution, e, as given by Eq. (A.5).

$$\beta = \frac{\ln e}{\ln^2 e + \pi^2} \tag{A.5}$$

References

Barrasso, D., Oka, S., Muliadi, A., Litster, J.D., Wassgren, C., Ramachandran, R., 2013a. Population balance model validation and prediction of CQAs for continuous milling processes: toward QbD in pharmaceutical drug product manufacturing. J. Pharm. Innovat. 8 (3), 147–162.

Barrasso, D., Ramachandran, R., 2012. A comparison of model order reduction techniques for a four-dimensional population balance model describing multi-component wet granulation processes. Chem. Eng. Sci. 80, 380–392.

Barrasso, D., Tamrakar, A., Ramachandran, R., May 2014. Model order reduction of a multi-scale PBM-DEM description of a wet granulation process via ANN. In: 7th World Congress on Particle Technology, Beijing, China.

Barrasso, D., Walia, S., Ramachandran, R., 2013b. Multi-component population balance modeling of continuous granulation processes: a parametric study and comparison with experimental trends. Powder Technol. 241, 85–97.

Behzadi, S.S., Klocker, J., Huttlin, H., Wolschann, P., Viernstein, H., 2005. Validation of fluid bed granulation utilizing artificial neural network. Int. J. Pharm. 291 (1/2), 139–148.

Biggs, C., Sanders, C., Scott, A., Willemse, A., Hoffman, A., Instone, T., Salman, A., Hounslow, M., 2003. Coupling granule properties and granulation rates in high-shear granulation. Powder Technol. 130 (1–3), 162–168.

Bilgili, E., Scarlett, B., 2005. Population balance modeling of non-linear effects in milling processes. Powder Technol. 153 (1), 59–71.

Borner, M., Peglow, M., Tsotsas, E., 2013. Derivation of parameters for a two compartment population balance model of Wurster fluidised bed granulation. Powder Technol. 238, 122–131.

Boukouvala, F., Gao, Y., Muzzio, F., Ierapetritou, M.G., 2013. Reduced-order discrete element method modeling. Chem. Eng. Sci. 95, 12–26.

Braumann, A., Kraft, M., Mort, P.R., 2010. Parameter estimation in a multidimensional granulation model. Powder Technol. 197 (3), 196–210.

Cameron, I., Wang, F., Immanuel, C., Stepanek, F., 2005. Process systems modelling and applications in granulation: a review. Chem. Eng. Sci. 60 (14), 3723–3750.

Capece, M., Bilgili, E., Dave, R., 2011. Identification of the breakage rate and distribution parameters in a non-linear population balance model for batch milling. Powder Technol. 208 (1), 195–204.

Chua, K.W., Makkawi, Y.T., Hounslow, M.J., 2013. A priori prediction of aggregation efficiency and rate constant for fluidized bed melt granulation. Chem. Eng. Sci. 98, 291–297.

Darelius, A., Brage, H., Rasmuson, A., Björn, I.N., Folestad, S., 2006. A volume-based multi-dimensional population balance approach for modelling high shear granulation. Chem. Eng. Sci. 61 (8), 2482–2493.

Darelius, A., Rasmuson, A., Bjorn, I.N., Folestad, S., 2005. High shear wet granulation modelling – a mechanistic approach using population balances. Powder Technol. 160 (3), 209–218.

DEM Solutions, 2013. EDEM 2.5 User Guide. DEM Solutions, Inc., Edinburgh, UK.

Dosta, M., Antonyuk, S., Heinrich, S., 2013. Multiscale simulation of agglomerate breakage in fluidized beds. Ind. Eng. Chem. Res. 52 (33), 11275–11281.

Dubey, A., Sarkar, A., Ierapetritou, M., Wassgren, C.R., Muzzio, F.J., 2011. Computational approaches for studying the granular dynamics of continuous blending processes, 1 – DEM based methods. Macromol. Mater. Eng. 296 (3/4), 290–307.

Freireich, B., Li, J., Litster, J., Wassgren, C., 2011. Incorporating particle flow information from discrete element simulations in population balance models of mixer-coaters. Chem. Eng. Sci. 66 (16), 3592–3604.

Fries, L., Antonyuk, S., Heinrich, S., Dopfer, D., Palzer, S., 2013. Collision dynamics in fluidised bed granulators: a DEM–CFD study. Chem. Eng. Sci. 86, 108–123.

Fries, L., Antonyuk, S., Heinrich, S., Palzer, S., 2011. DEM–CFD modeling of a fluidized bed spray granulator. Chem. Eng. Sci. 66 (11), 2340–2355.

Gantt, J.A., Cameron, I.T., Litster, J.D., Gatzke, E.P., 2006. Determination of coalescence kernels for high-shear

granulation using DEM simulations. Powder Technol. 170 (2), 53–63.
Gantt, J.A., Gatzke, E.P., 2006. A stochastic technique for multidimensional granulation modeling. AIChE J. 52 (9), 3067–3077.
Gao, Y., Ierapetritou, M., Muzzio, F., 2011. Periodic section modeling of convective continuous powder mixing processes. AIChE J. 58 (1), 69–78.
Gerstlauer, A., Motz, S., Mitrovic, A., Gilles, E.-D., 2002. Development, analysis and validation of population models for continuous and batch crystallizers. Chem. Eng. Sci. 57 (20), 4311–4327.
Glaser, T., Sanders, C.F., Wang, F., Cameron, I.T., Litster, J.D., Poon, J.M.-H., Ramachandran, R., Immanuel, C.D., Doyle III, F.J., 2009. Model predictive control of continuous drum granulation. J. Process Control 19 (4), 615–622.
Goldschmidt, M., Weijers, G., Boerefijn, R., Kuipers, J., 2003. Discrete element modelling of fluidised bed spray granulation. Powder Technol. 138 (1), 39–45.
Hassanpour, A., Kwan, C., Ng, B., Rahmanian, N., Ding, Y., Antony, S., Jia, X., Ghadiri, M., 2009. Effect of granulation scale-up on the strength of granules. Powder Technol. 189 (2), 304–312.
Hounslow, M.J., Pearson, J.M.K., Instone, T., 2001. Tracer studies of high-shear granulation: II. Population balance modeling. AIChE J. 47 (9), 1984–1999.
Iveson, S., Litster, J., Ennis, B., 1996. Fundamental studies of granule consolidation, Part 1: Effects of binder content and binder viscosity. Powder Technol. 88 (1), 15–20.
Iveson, S.M., 2002. Limitations of one-dimensional population balance models of wet granulation processes. Powder Technol. 124 (3), 219–229.
Iveson, S.M., Litster, J.D., Hapgood, K., Ennis, B.J., 2001. Nucleation, growth and breakage phenomena in agitated wet granulation processes: a review. Powder Technol. 117 (1/2), 3–39.
Jajcevic, D., Siegmann, E., Radeke, C., Khinast, J.G., 2013. Large-scale CFD–DEM simulations of fluidized granular systems. Chem. Eng. Sci. 98, 298–310.
Kafui, K., Thornton, C., 2000. Numerical simulations of impact breakage of a spherical crystalline agglomerate. Powder Technol. 109 (1–3), 113–132.
Li, J., Freireich, B.J., Wassgren, C.R., Litster, J.D., 2013. Experimental validation of a 2-D population balance model for spray coating processes. Chem. Eng. Sci. 95, 360–365.
Lian, G., Thornton, C., Adams, M.J., 1998. Discrete particle simulation of agglomerate impact coalescence. Chem. Eng. Sci. 53 (19), 3381–3391.
Liu, L.X., Litster, J.D., 2002. Population balance modelling of granulation with a physically based coalescence kernel. Chem. Eng. Sci. 57 (12), 2183–2191.
Madec, L., Falk, L., Plasari, E., 2003. Modelling of the agglomeration in suspension process with multidimensional kernels. Powder Technol. 130 (1–3), 147–153.
Maronga, S., Wnukowski, P., 1997. Modelling of the three-domain fluidized-bed particulate coating process. Chem. Eng. Sci. 52 (17), 2915–2925.
Marshall Jr., C.L., Rajniak, P., Matsoukas, T., 2011. Numerical simulations of two-component granulation: comparison of three methods. Chem. Eng. Res. Des. 89 (5), 545–552.
Marshall Jr., C.L., Rajniak, P., Matsoukas, T., 2012. Multi-component population balance modeling of granulation with continuous addition of binder. Powder Technol. 236, 211–220.
Matsoukas, T., Kim, T., Lee, K., 2009. Bicomponent aggregation with composition-dependent rates and the approach to well-mixed state. Chem. Eng. Sci. 64 (4), 787–799.
Matsoukas, T., Marshall Jr., C.L., 2010. Bicomponent aggregation in finite systems. Europhys. Lett. 92 (4), 46007.
Pandey, P., Tao, J., Chaudhury, A., Ramachandran, R., Gao, J.Z., Bindra, D.S., 2013. A combined experimental and modeling approach to study the effects of high-shear wet granulation process parameters on granule characteristics. Pharm. Dev. Technol. 18 (1), 210–224.
Pandya, J., Spielman, L., 1983. Floc breakage in agitated suspensions: effect of agitation rate. Chem. Eng. Sci. 38 (12), 1983–1992.
Pinto, M.A., Immanuel, C.D., Doyle III, F.J., 2007. A feasible solution technique for higher-dimensional population balance models. Comput. Chem. Eng. 31 (10), 1242–1256.
Poon, J.M.-H., Immanuel, C.D., Doyle III, F.J., Litster, J.D., 2008. A three-dimensional population balance model of granulation with a mechanistic representation of the nucleation and aggregation phenomena. Chem. Eng. Sci. 63 (5), 1315–1329.
Poon, J.M.-H., Ramachandran, R., Sanders, C.F., Glaser, T., Immanuel, C.D., Doyle III, F.J., Litster, J.D., Stepanek, F., Wang, F.-Y., Cameron, I.T., 2009. Experimental validation studies on a multi-dimensional and multi-scale population balance model of batch granulation. Chem. Eng. Sci. 64 (4), 775–786.
Ramachandran, R., Barton, P.I., 2010. Effective parameter estimation within a multi-dimensional population balance model framework. Chem. Eng. Sci. 65 (16), 4884–4893.
Ramachandran, R., Chaudhury, A., 2012. Model-based design and control of a continuous drum granulation process. Chem. Eng. Res. Des. 90 (8), 1063–1073.
Ramachandran, R., Immanuel, C.D., Stepanek, F., Litster, J.D., Doyle III, F.J., 2009. A mechanistic model for breakage in population balances of granulation: theoretical kernel development and experimental validation. Chem. Eng. Res. Des. 87 (4), 598–614.
Ramachandran, R., Poon, J.M.-H., Sanders, C.F.W., Glaser, T., Immanuel, C.D., Doyle III, F.J., Litster, J.D., Stepanek, F., Wang, F.-Y., Cameron, I.T., 2008. Experimental studies on distributions of granule size, binder content and porosity in batch drum granulation: inferences on process modelling requirements and process sensitivities. Powder Technol. 188 (2), 89–101.
Ramkrishna, D., 2000. Population Balances: Theory and Applications to Particulate Systems in Engineering. Academic Press, San Diego.
Ranjbarian, S., Farhadi, F., 2013. Evaluation of the effects of process parameters on granule mean size in a conical high shear granulator using response surface methodology. Powder Technol. 237, 186–190.
Reinhold, A., Briesen, H., 2012. Numerical behavior of a multiscale aggregation model – coupling population balances and discrete element models. Chem. Eng. Sci. 70, 165–175.
Scott, A., Hounslow, M., Instone, T., 2000. Direct evidence of heterogeneity during high-shear granulation. Powder Technol. 113 (1/2), 205–213.
Sen, M., Ramachandran, R., 2013. A multi-dimensional population balance model approach to continuous powder mixing processes. Adv. Powder Technol. 24 (1), 51–59.
Sen, M., Singh, R., Vanarase, A., John, J., Ramachandran, R., 2012. Multi-dimensional population balance modeling and experimental validation of continuous powder mixing processes. Chem. Eng. Sci. 80, 349–360.
Stepanek, F., Rajniak, P., Mancinelli, C., Chern, R., Ramachandran, R., 2009. Distribution and accessibility of binder in wet granules. Powder Technol. 189 (2), 376–384.
Tan, H., Goldschmidt, M., Boerefijn, R., Hounslow, M., Salman, A., Kuipers, J., 2004. Building population balance model for fluidized bed melt granulation: lessons from kinetic theory of granular flow. Powder Technol. 142 (2/3), 103–109.
Tardos, G.I., Khan, M.I., Mort, P.R., 1997. Critical parameters and limiting conditions in binder granulation of fine powders. Powder Technol. 94 (3), 245–258.
Verkoeijen, D., Pouw, G.A., Meesters, G.M.H., Scarlett, B., 2002. Population balances for particulate processes – a volume approach. Chem. Eng. Sci. 57 (12), 2287–2303.
Vervaet, C., Remon, J.P., 2005. Continuous granulation in the pharmaceutical industry. Chem. Eng. Sci. 60 (14), 3949–3957.

Wang, F.Y., Cameron, I.T., 2002. Review and future directions in the modelling and control of continuous drum granulation. Powder Technol. 124 (3), 238–253.

Wang, M., Yang, R., Yu, A., 2012. DEM investigation of energy distribution and particle breakage in tumbling ball mills. Powder Technol. 223, 83–91.

Wauters, P., 2001. Modeling and mechanisms of granulation. Delft University of Technology, Delft, The Netherlands (Ph.D. thesis).

Yu, L.X., 2008. Pharmaceutical quality by design: product and process development, understanding, and control. Pharm. Res. 25 (4), 781–791.